Balancing Impedance and Controllability in Response Reconstruction

Matthew J. Tuman
Undergraduate Research Assistant; UW-Madison – Department of Engineering Physics
tuman@wisc.edu

Matthew S. Allen
Professor; Brigham Young University – Mechanical Engineering Department
matt.allen@byu.edu

Washington J. DeLima, Eric Dodgen & Jonathan Hower
Honeywell Federal Manufacturing & Technologies
wdelima@kcnsc.doe.gov, edodgen@kcnsc.doe.gov & jhower@kcnsc.doe.gov

ABSTRACT

One concept in smart dynamic testing is to match the impedance that a component experiences between test and the environment of interest, but this begs the question: how much of an impedance match is needed and could there be too much? In a prior work, the authors performed MIMO testing with a small component connected to various assemblies, each of which had a differing degree of similarity to the actual flight boundary conditions. The results showed that the fidelity of the response at locations away from the control accelerometers was highly sensitive to the impedance. This work presents further case studies to explore these ideas. Subsequent tests are presented for an assembly that presumably matched the impedance even better, and which was also much more flexible, and the results obtained are even worse than when no attention was given to the impedance. Hence, the work presented here suggests that one should seek a balance between 1.) matching the impedance and 2.) improving the controllability of the component of interest. The concepts are explored using both test data of a benchmark component, for which the environment of interest was recorded as the component flew on a sounding rocket.

Keywords: Shaker Test, Operational Vibration Environment, Substructuring, Force Reconstruction

1. Introduction

Response reconstruction tests aim to determine whether a newly designed parts can survive their intended operational environment. Typically, this test is performed using a single-axis shaker controlling to one accelerometer on the part of interest in a closed loop [1]. Although this methodology has been standard for many years, there are a few challenges that require solutions. First, each axis is excited individually. This requires extra time and expense to perform the test, and increased handling of the hardware, which can increase the probability of damage occurring. However, an even more significant concern is that these tests ignore any off-axis motion; while

the test may be successfully controlling the accelerometer in the axis of excitation, the part may be subjected to motion in the other directions that is much more severe than the operational environment. Another issue in any kind of shaker testing is that the dynamics of the part change when the shaker is attached (i.e. there is an impedance mismatch at the interface), and often this causes the part to respond at its resonances at much higher amplitudes than would be observed in the operational environment. This over-testing causes many failures to occur during shaker testing that would not occur during operation, and huge expense can be incurred either to redesign the parts or to retest the parts using more conservative environments.

Engineers have known since the 1970's that the impedance mismatch between the shaker test and the operational environment can cause severe over-testing [2], and although some methods exist for addressing this, they all have significant limitations and none have been universally embraced. Many of the available methods are summarized in Figure 1.
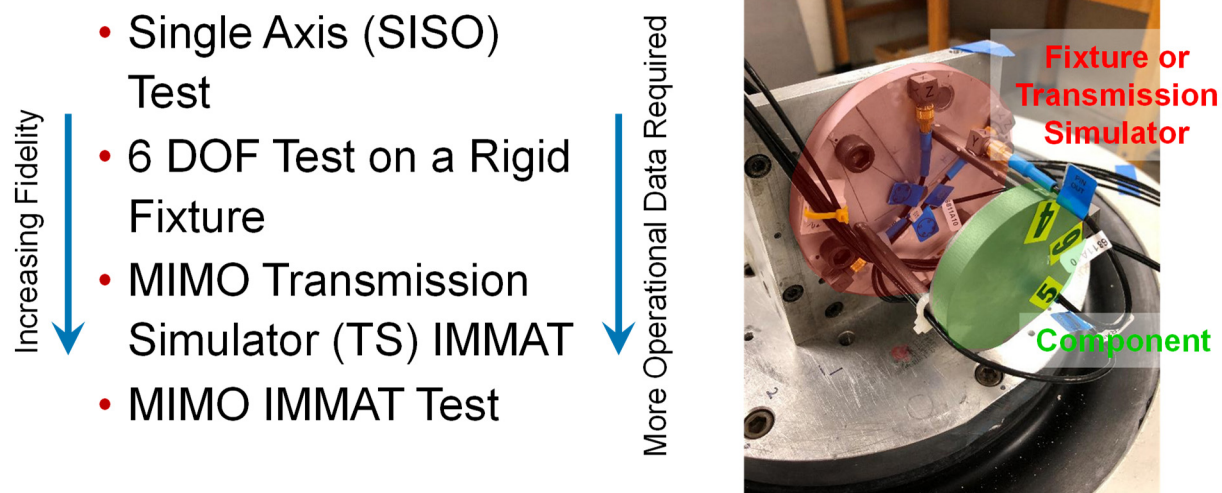

Figure 1: *Various methods have been proposed for dynamic environment testing, each of which has differing fidelity and knowledge of the operational environment.*

Six-degree-of-freedom (6DOF) shaker tables using multi-input-multi-output (MIMO) control have been built [3]. These impressive shakers are able to control multiple degrees of freedom in multiple directions simultaneously, addressing some of the issues outlined above with SISO testing. However, the component under test is still required to be bolted to a massive shaker table, so it is typically difficult to match the impedance. Furthermore, the method loses fidelity if the flexible modes of the table are in the frequency range of interest. At the other end of the spectrum, in terms of fidelity, is the Impedance-Matched-Multi-Axis-Testing (IMMAT) methodology [4]. This technique also excites the component in all directions using MIMO control and yet rather than using one massive shaker table, it advocates for using fixturing that mimics the boundary conditions that the part experiences in operation. In the trials to date this method has recreated dynamic environments far more accurately than single-axis testing [4], [5], yet it presumes that one has enough measurements from the component of interest in the operational environment to determine its modal motion. Specifically, to perform IMMAT on the component shown in Figure 1, one would need to have operational measurements on the fixturing (highlighted red) as well as the component (highlighted green).

In order to obtain a compromise between these approaches, in terms of the fidelity and the data that is required, the authors proposed the Transmission Simulator IMMAT approach (TS-

IMMAT) [6], in which control is only applied to the fixture or transmission simulator (i.e. the part highlighted red in Figure 1), and one then relies on a good impedance match between the operation and test environments to achieve an accurate reconstruction of the response on the component of interest. This work presents a few improvements to this method and studies the method using representative hardware and environment data to understand its advantages and limitations.

Before proceeding, it is worth mentioning two other approaches that are frequently used to address the impedance mismatch. When data on the component (green in Figure 1) is available, one can set response limits, in essence telling the shaker system to reproduce the environment as closely as it can without exceeding those limits. The idea is similar in force limiting [2], [7], although in that case load cells are used between the part and the shaker and the reaction forces are limited. There are some advantages, as the reaction force limits can be estimated using effective mass principles, although several practitioners have found that having load cells connected between the part can be problematic; it introduces additional joints whose preloads are limited by the strength of the force gauges and hence the joints may slip and change the dynamics during the test. (For a comprehensive reference see [8] and see [9] for a case study showing the behavior of industrial joints at typical preloads.) Recently, Van Fossen and Napolitano [10] presented an alternative in which the connection forces are estimated from accelerometer measurements, in essence presenting a hybrid between force and response limiting methods. Any of these methods could prove very effective as long as: 1.) reasonable limits are known and 2.) using those limits does not degrade the accuracy of the environment too much.

Returning to the TS-IMMAT approach, prior work has suggested that improving the impedance of the transmission simulator (TS) will lead to a more accurate reconstruction of the operational environment for the uncontrolled component [11]. Additionally, this previous investigation found that MIMO simulations based on frequency response functions (FRF's) from a modal pretest can do a reasonable job of predicting response reconstruction accuracy for physical MIMO test. To investigate this further, this work presents tests and simulations showing the accuracy with which the response is reconstructed when more of the operational structure is included (i.e. a next-level assembly is used as the TS). Furthermore, to better predict the accuracy of a MIMO test, a condition number threshold is implemented in the simulations to mimic the physical controller that is used in test. This is a continuation of [6][11][12].

2. Assembly and Environment Definitions

The next-level assembly under test is shown in Figure 2. Previous work performed reconstruction tests using assemblies with the same plate (TS) and stool (subcomponent); however, these assemblies did not include the pillars or the bottom bulkhead [11]. The accelerometers are positioned in a cylindrical coordinate system, and the directions referenced throughout the rest of this analysis are specified in Figure 2.

This assembly flew inside a sounding rocket flown for Kansas City National Security Campus in July 2019. The assembly was instrumented with three triaxial on the plate, and three triaxial accelerometers on the stool. During flight, the rocket experienced four main phases: boost, coast, deployment of the drogue parachute, and deployment of the main parachute. The operational environment power spectral density (PSD) profiles are constructed from acceleration time data from 0.5 to 20 seconds after launch. This time frame captures the boost and coast phase while excluding any shock event at ignition along with the deployment of the parachutes.
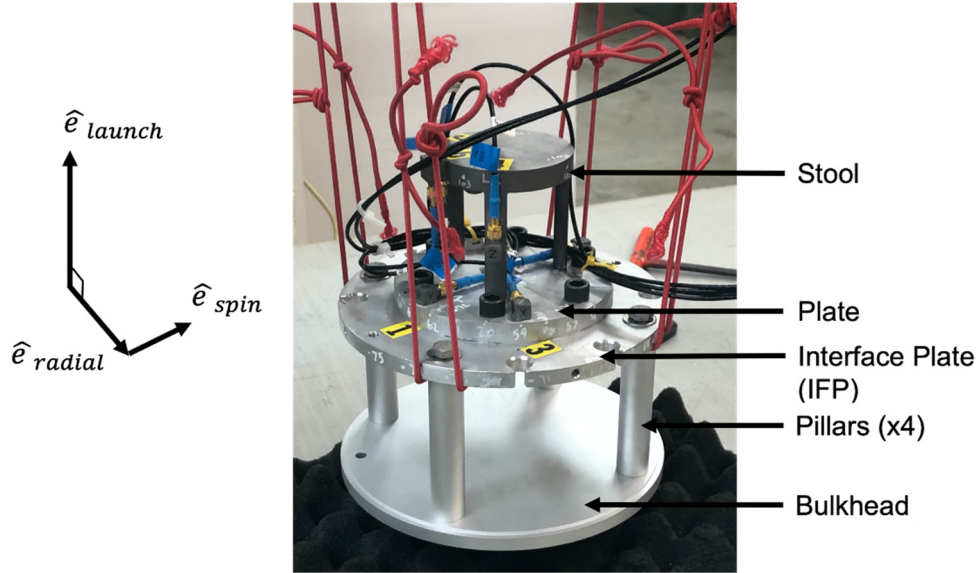
Figure 2: The instrumented next-level assembly

The frequency spacing of the PSD profiles generated is 0.8206 Hz, and the testing bandwidth of interest is 100 to 5000 Hz. Unfortunately, the data from the first accelerometer in the radial direction (channel 1) only recorded noise during flight. Thus, there are eight channels on the plate and nine channels on the stool that recorded useful data.

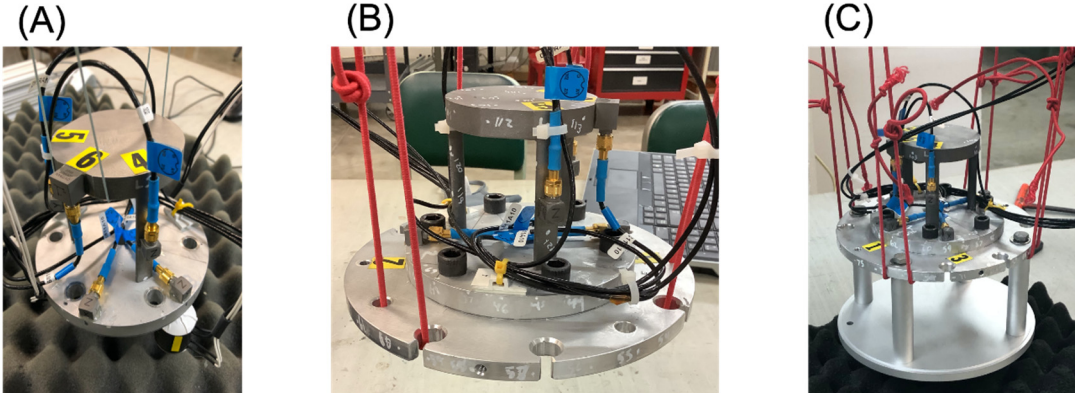Three assemblies will be considered in the following analysis and are illustrated in Figure 3.

Figure 3: The three assemblies tested are Configuration A with the stool and plate, Configuration B with the stool, plate, and IFP, and Configuration C with the stool, plate, IFP, pillars, and bulkhead

For each configuration, the goal is to reconstruct the environment on the plate using six small shakers using MIMO control. To assess the success of a TS-IMMAT test for each configuration, the accuracy of the controlled reconstructed plate response and the accuracy of the uncontrolled stool response will be compared. Our prior work [11] presented TS-IMMAT reconstruction tests on Configurations A and B; this work will focus on comparing those with Configuration C.

3. MIMO Simulations

The accuracy of MIMO reconstruction tests using the TS approach was found to be sensitive to the forcing input location of the shakers. Because each experimental setup requires a

significant amount of time, a process was devised to determine optimal forcing input locations by running multiple MIMO tests in simulation. This procedure required frequency response functions (FRF's) between all the possible shaker input locations and the accelerometers on the component under test.

3.1. Roving Hammer FRF's

A modal roving hammer test was performed on Configuration C. This physical test constructed a comprehensive FRF matrix relating eighty-two forcing inputs to the eighteen accelerometer channels on the assembly. Data Physics Abacus hardware and SignalCalc 730 software recorded the FRF's in the bandwidth of 0 to 5250 Hz with a frequency resolution 0f 0.82 Hz to match the environmental acceleration profiles. Forty-one forcing inputs were recorded on the interface plate with thirty in the launch direction and eleven in the radial direction. Each pillar was characterized using three inputs in the spin direction and two in the radial direction. Lastly, fifteen inputs were applied on the bottom bulkhead in the launch direction and six inputs were recorded in the radial direction. These FRFs could be used to simulate eighty-two potential shaker locations.

3.2. Mathematical Model

Derived from a linear vibration model, the spectral density of the response $S_{XX}(\omega)$ of an n degree of freedom (DOF) system in the frequency domain at a specific frequency, ω can be computed from a forcing input PSD matrix of d inputs, $S_{FF}(\omega)$, the FRF matrix relating inputs to an outputs, $H_{XF}(\omega)$, and the Hermitian of the FRF, $H_{XF}^*(\omega)$, as presented in Equation **Error! Reference source not found.**.

$$S_{XX}(\omega) = H_{XF}(\omega) \cdot S_{FF}(\omega) \cdot H_{XF}^*(\omega) \tag{1}$$

The dimension of $S_{XX}(\omega)$ is $(n \times n)$, $S_{FF}(\omega)$ is $(d \times d)$, and $H_{XF}(\omega)$ is $(n \times d)$. If the operational environment, or PSD matrix $(S_{XX}(\omega))$ is known, Equation **Error! Reference source not found.** can be inverted to solve for the forcing input PSD matrix, $S_{FF,est}(\omega)$, using Equation 2. If an overdetermined system is present, where there are more DOF than forcing inputs ($n > d$), the pseudoinverse of the FRF, denoted $H_{XF}^+(\omega)$, can be used to find the forcing input that minimizes least squares error.

$$S_{FF,est}(\omega) = H_{XF}^+(\omega) \cdot S_{xx}(\omega) \cdot \left(H_{XF}^*(\omega)\right)^+ \tag{2}$$

Using this least squares solution for the estimated forcing input, one can then solve for the estimated response, $S_{XX,est}(\omega)$, using Equation 3.

$$S_{XX,est}(\omega) = H_{XF}(\omega) \cdot S_{FF,est}(\omega) \cdot H_{XF}^*(\omega) \tag{3}$$

Because FRF's are recorded from the modal hammer test and the operational acceleration PSD profiles are known, Equation 2 and Equation 3 can be used to simulate a MIMO test. To simulate various forcing inputs, the columns of $H_{XF}^+(\omega)$ are trimmed to only correspond to the inputs of interest (no more than six in this work). Also, $S_{xx}(\omega)$ is trimmed to include only the eight control accelerometers on the plate. This response PSD matrix contains diagonal and off diagonal measurements.

3.3. Shaker Selection Algorithm
To determine a near optimal set of shaker locations for the best reconstruction accuracy, the shaker placement algorithm from [13] was adapted. Additionally, to evaluate the success of a MIMO simulation, an error metric from [13] was also used. First, the average dB difference of two ASDs for all relevant accelerometer channels at a frequency line is computed using Equation **Error! Reference source not found.**.

$$e_{ASD}(f_i) = \sqrt{\frac{1}{n_{accels}} \sum_{k=1}^{n_{accels}} \left[dB[S_{X_k X_k}(f_i)] - dB[S_{X_k X_k, lab}(f_i)]\right]^2} \qquad (4)$$

For this work, $S_{X_k X_k, lab}$ is the simulated or experimental acceleration ASD for the kth accelerometer DOF and $S_{X_k X_k}$ is the operational ASD for the same DOF. After computing an error value for each frequency line, a final metric is computed using Equation **Error! Reference source not found.**.

$$e_{ASD} = \sqrt{\frac{1}{n_{freq}} \sum_{i=1}^{n_{freq}} e_{ASD}(f_i)^2} \qquad (5)$$

This final error number represents the average dB error across all accelerometers and frequency line. A low error metric communicates a successful reconstruction test and will be used moving forward to compare various tests. With the error metric defined, the shaker location algorithm is as follows:
1) Start with a pool of all possible forcing input locations from the roving hammer test of Configuration C
2) Simulate the MIMO response for each forcing input location in the remaining pool (controlling to the eight plate accelerometers)
3) Keep the forcing input location that produces the lowest error on the controlled DOF (plate accelerometers) and remove it from the pool of possible locations
4) Add this kept forcing input location to the set of forcing locations.
5) Repeat steps 2-4 with the kept forcing input location/s from the previous iterations plus each candidate location and again keep the best candidate location until the number of desired shakers is reached.

To remain consistent with the prior work [11], the optimization stopped once it determined the six best shaker locations for Configuration C.

4. Methodology

The workflow for performing the TS-IMMAT reconstruction test was as follows. As mentioned previously, a modal roving hammer test was performed on the next-level assembly (Configuration C) with eighty-two forcing inputs recorded. Then, using MIMO simulations and the shaker selection algorithm, optimal shaker input locations were determined. Shakers were then attached at these locations. Three SIEMENS Q-MSH electromagnetic (EM) inertial shakers were used to excite the assembly under test in the launch direction. These three shakers were attached directly to the structure using super glue. In the off-launch directions, two APS 300 EM shakers and one LDS 203 EM were connected to the assembly via stingers made of piano wire which were also attached with super glue. The experimental setup with optimal shaker inputs is presented in Figure 4.
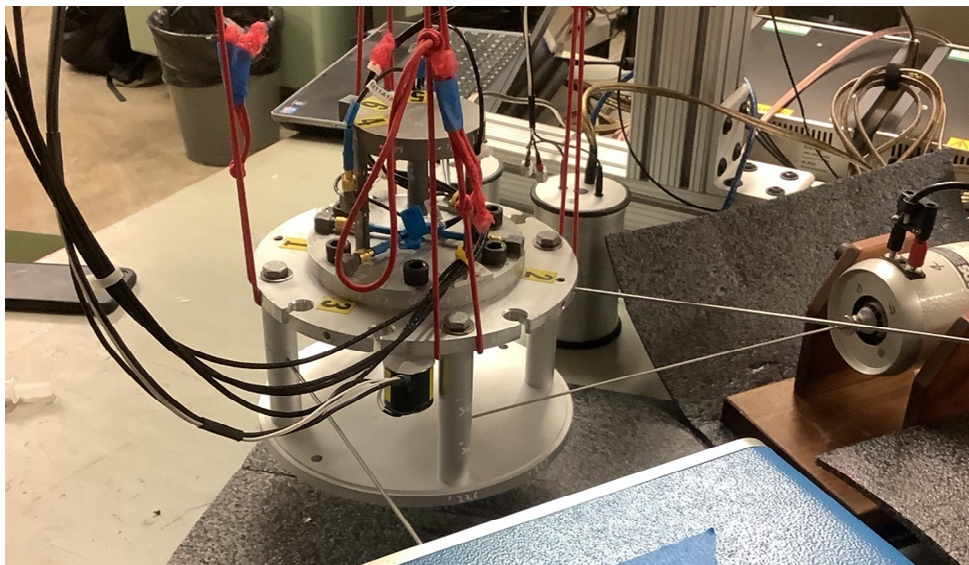

Figure 4: Experimental setup for MIMO reconstruction test of next-level assembly (Configuration C)

To perform the MIMO test, Data Physics Abacus hardware and Data Physics SignalStar Matrix controller software were used. Per requirements of the TS-IMMAT approach, the closed-loop MIMO software only controlled to the accelerometers on the plate. Because one accelerometer channel recorded noisy data during flight and another channel started to record poor measurements in the laboratory, only seven accelerometer channels were controlled to. The control profiles were the PSD matrices constructed from the flight data as described in Section 2. The remaining 9 accelerometer channels on the stool were not controlled to, but they were measured.

5. MIMO Reconstruction

Following the methodology provided, a TS-IMMAT response reconstruction test was performed. To visualize the accuracy of this test, Figure 5 presents the auto-spectral densities (ASD's) for the accelerometer channels on the controlled plate. The black line is the operational environment profile that is being controlled to, the blue line is the response recorded during the reconstruction test, and the red lines are a plus or minus 6dB error envelope of the operational profile. Additionally, for each channel, the dB error is provided in each subplot's title.
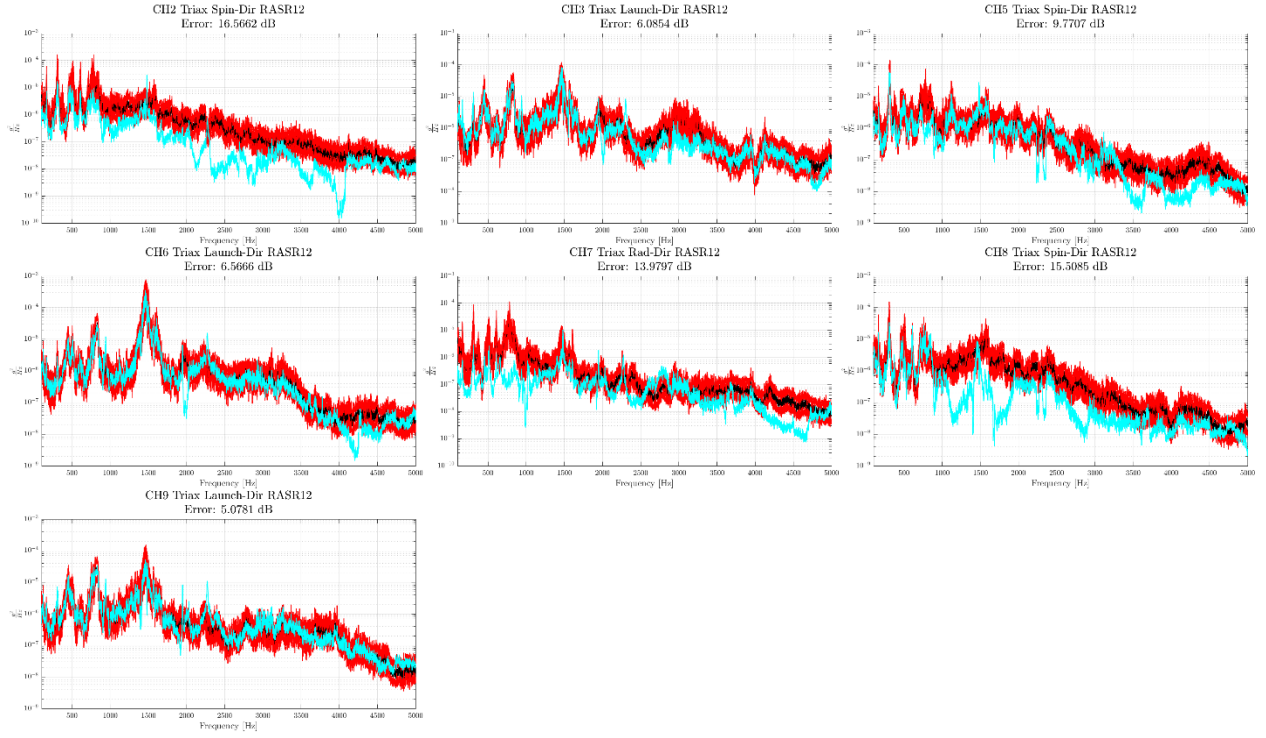
Figure 5*: Reconstruction ASDs of the controlled accelerometers on the plate (blue) along with the control ASDs (black) and a ±6dB control error envelope (red)*

The reconstruction in the launch direction (channels 3, 6, and 9) was very accurate in the full testing bandwidth with error values hovering around 6dB. On the other hand, reconstruction accuracy in the off-launch directions is poor with significant undertesting occurring in the spin direction on channels 2 and 8. This inability to generate the desired response in the off-launch directions leads to a relatively higher error for the plate of 11.4dB.

In practice we presume that one would not have measurements on the component of interest, but in these tests we did have accelerometers on the stool so we could evaluate the performance of the proposed TS-IMMAT approach. Turning our attention now to the uncontrolled stool, Figure 6 illustrates the measured ASD's of the accelerometer channels on the stool (blue) with the environment profiles generated from the flight data (black).
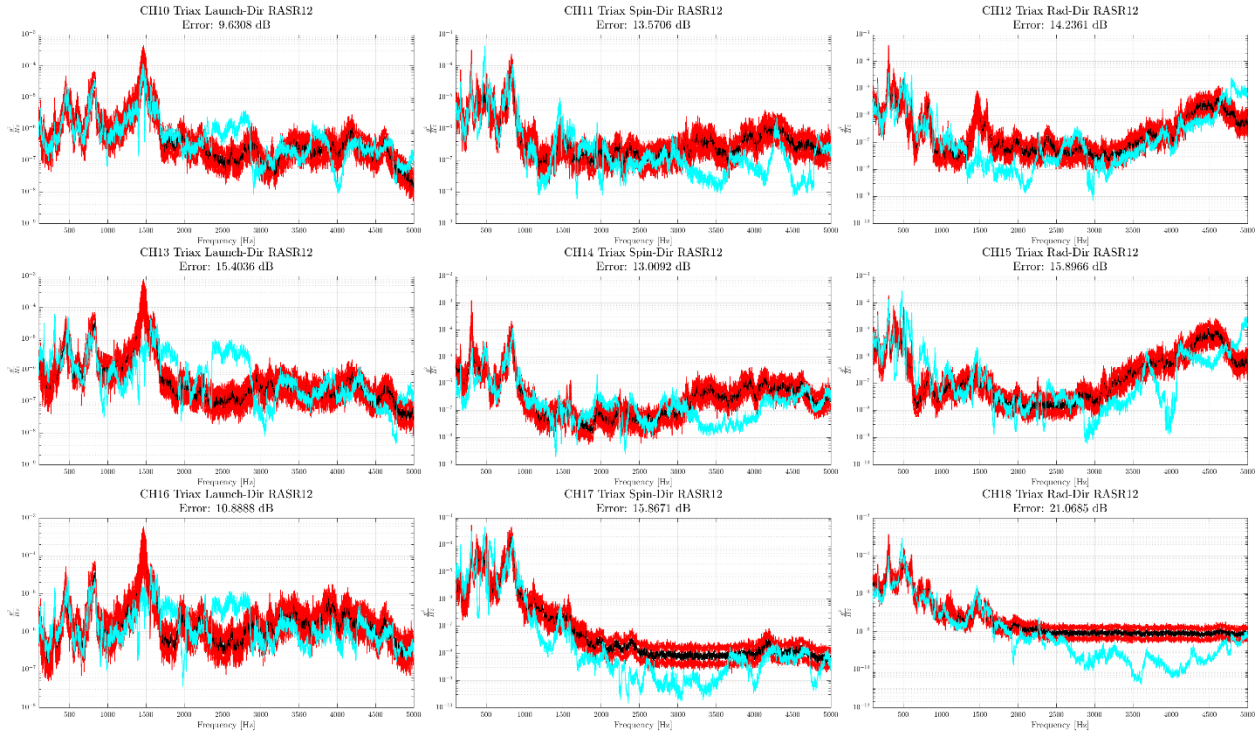
Figure 6*: Measured ASDs of the uncontrolled accelerometers on the stool (blue) along with the environment ASDs (black) and a ±6dB environment error envelope (red)*

Once again, the measured responses in the launch direction (channels 10, 13, and 16) are the most accurate, presumably because the response on the TS was best controlled in this axis of excitation. As might have been expected, because control was significantly worse on the plate in the off-axis directions, the measured responses of the stool in these directions are also worse on average, although not significantly worse than the launch direction. In fact, there are three channels in the off-launch directions (11, 12 and 14) that have a lower error metric than channel 13 in the launch direction. Nonetheless, reconstruction accuracy of this uncontrolled subcomponent was still unsatisfactory with an overall error of 14.7dB.

Next, with TS-IMMAT reconstruction tests performed on Configuration A, Configuration B, and now Configuration C, the accuracy for each assembly can be assessed quantitatively using the dB error metric. Table 1 presents the error metric from 100 to 2000 Hz and 100 to 5000 Hz for the three assemblies tested.

Table 1*: Error in experimental reconstruction for three assemblies tested*

Assembly	Error from 100-2000 Hz (dB)		Error from 100-5000Hz (dB)	
	Plate	*Stool*	*Plate*	*Stool*
Configuration A	9.2	12.3	8.9	15.7
Configuration B	7.5	11.4	7.7	12.8
Configuration C	11.7	12.4	11.4	14.7

The previous testing of Configuration A and Configuration B suggested that using more of the original operational structure improves the response accuracy for the controlled transmission

simulator (plate) and for the uncontrolled subcomponent (stool). Because Configuration B is more similar to the operational structure than Configuration A, Configuration B was presumed to have a better impedance match. However, Configuration C includes even more of the operational structure than the other two assemblies and therefore should best match the impedance.

The discovery that Configuration C does not have improved reconstruction accuracy presents some interesting implications that must be explored moving forward. One theory was that the transmission simulator is far more flexible in Configuration C, and that this may contribute to the difficulty. Because the stool remained the same in each test, the flexibility of the various transmission simulators can be compared by comparing the number of modes of the assembly that are within the bandwidth of interest for each configuration. This is summarized in Table 2.

Table 2: Number of flexible modes below 5000 Hz for each configuration.

Assembly	Modes
Configuration A	9
Configuration B	9
Configuration C	21

Because the number of forcing inputs was the same between tests, one would expect that the system with fewer modes will be more controllable, and this could explain why the results degraded for Configuration C. The authors are exploring metrics or concepts that can be used to quantify the difficulty of controlling a particular assembly, and this may help in quantifying these effects. In any event, this study has shown that the ideal test may not simply involve the best possible impedance match but may also need to consider controllability.

With regards to the impedance match, more objective metrics are needed to quantify impedance so one can specify what level of matching is needed. The term impedance matching has been loosely used in this work as an evaluation of how similar the dynamics are between the assembly under test and the assembly during operation. However, there has been no quantitative formulation for this metric, and it has been assumed that more of the original structure guarantees a better match. Configuration C introduces numerous flexible modes of the pillars and the bottom bulkhead, but during operation, there was a casing around the assembly which may drastically change the contribution of these modes to the operational response. Thus, the impedance match of Configuration C may actually be worse than that in Configuration B. Until a more rigorous metric can be developed, caution must be used when assuming that a next level assembly ensures better an impedance match and thus more accurate reconstruction results.

Lastly, circling back to the transmission simulator methodology, the reconstruction accuracy is predicated on the transmission simulator spanning the modal space that is present during the operational response. Therefore, if the subcomponent has no input other than the TS, when the modal response of the TS is reconstructed, the response of the subcomponent should also be recreated. However, with all three configurations exhibiting degradation of response accuracy between the TS (plate) and subcomponent (stool), it does not appear as if the TS is perfectly spanning the operational modal space. Although this is not entirely surprising, the results from these three configurations suggest that more time should be spent determining the highest contributing modes in operation. Perhaps the modal space spanned by Configuration B is more representative of the response space than Configuration C, and therefore it is more accurate. It does seem important to first determine the dominant operational modes and to design a

transmission simulator that captures them; this is currently being explored but will not be reported here.

6. Simulation with Condition Number Threshold

As mentioned previously, MIMO simulations are very important in the workflow and have been used to reliably determine forcing inputs for the three assemblies tested. While the MIMO simulations have been useful for finding optimal input locations and can predict which configuration of next-level assembly will have better accuracy for the uncontrolled subcomponent [11], in most cases to date they have predicted that reconstruction accuracy on the controlled TS (plate) should be much better than what is achieved in experiment. For instance, in simulation we are consistently able to achieve an error of 3dB on the plate accelerometers for Configurations A and B, but during actual experiments, this control error is typically between 7dB and 10dB. Although the Data Physics control software is proprietary, it is known that a condition number threshold is utilized to limit force input magnitudes that may exceed shaker capabilities. Thus, this section will explore how to implement a condition number in simulation and compare simulated results with and without a condition number threshold used.

6.1. Condition Number Threshold Implementation

A condition number threshold is traditionally used when inverting ill-conditioned matrices to limit the magnitude of elements in the inverse. In the MIMO simulation theory, an inversion only takes place in Equation 2 when solving for $S_{FF,est}(\omega)$. The following procedure is used to compute the pseudoinverse of the FRF, $H_{XF}^+(\omega)$. First, the FRF, $H_{XF}(\omega)$, is decomposed using the singular value decomposition (SVD). In this derivation, it is assumed there are n outputs and d inputs where d is less than n.

$$H_{XF}(\omega) = U\Sigma V^T \tag{6}$$

Here, Σ is a matrix containing the singular values of the decomposition as shown in Equation 7.

$$\Sigma = \begin{bmatrix} \sigma_1^2 & 0 & 0 \\ 0 & . & 0 \\ 0 & 0 & \sigma_d^2 \end{bmatrix} \tag{7}$$

As a property of the SVD, the singular values are ordered by magnitude with the largest singular value being σ_1. Next, we define our condition number, c_i, for each singular value using Equation 8.

$$c_i = \frac{\sigma_i^2}{\sigma_1^2} \tag{8}$$

With a threshold value defined, $c_{threshold}$, the index k is found by satisfying the condition in Equation 9.

$$c_k > c_{threshold} > c_{k+1} \tag{9}$$

Then, a truncated k rank approximation of the pseudoinverse FRF is computed using Equation 10.

$$\boldsymbol{H}_{XF}^+(\omega) = \sum_{i=1}^{k} \frac{1}{\sigma_i^2} \boldsymbol{V}_i \boldsymbol{U}_i^T \tag{10}$$

6.2. Simulation Results with Condition Number Threshold

To evaluate the effect of the condition number threshold on MIMO control, each physical experiment presented in Table 1 was repeated in simulation with the threshold and without the threshold. The threshold in simulation matches that which was used in experiment; these values ranged from 0.02 to 0.05. Table 3 presents the errors for each configuration in the format of *Simulation without Threshold / Simulation with Threshold / Physical Experiment*.

Table 3: Reconstruction accuracy error for the three configurations tested (Simulation without Threshold / Simulation with Threshold / Physical Experiment)

Assembly	Plate Error 100-5000 Hz (dB)	Stool Error 100-5000 Hz (dB)
Configuration A	3.4 / 5.2 / 8.9	11.6 / 14.9 / 15.7
Configuration B	2.3 / 5.0 / 7.7	16.1 / 12.0 / 12.8
Configuration C	5.6/ 7.01 / 11.4	12.1 / 11.4 / 14.7

For all three configurations, the errors on the plate are more similar between physical test and simulation when the condition number threshold is used. This is also the case for Configuration A and Configuration B on the stool. Therefore, these results suggest that a condition number threshold improves the ability of a simulation to predict what will occur during a physical test.

The question that now arises is why this threshold makes the simulation more realistic. Looking at Equation 10, small values of σ_i^2 can dramatically increase the magnitude of $\boldsymbol{H}_{XF}^+(\omega)$. If a large magnitude $\boldsymbol{H}_{XF}^+(\omega)$ is then used in Equation 2, the magnitude of the forcing input, $\boldsymbol{S}_{FF,est}(\omega)$, will also increase. This is visualized in Figure 7 where the simulated forcing input ASD's for Configuration B with a threshold (blue) and without a threshold (purple). Additionally, the rank of $\boldsymbol{H}_{XF}^+(\omega)$ is plotted (orange) on the right axis.
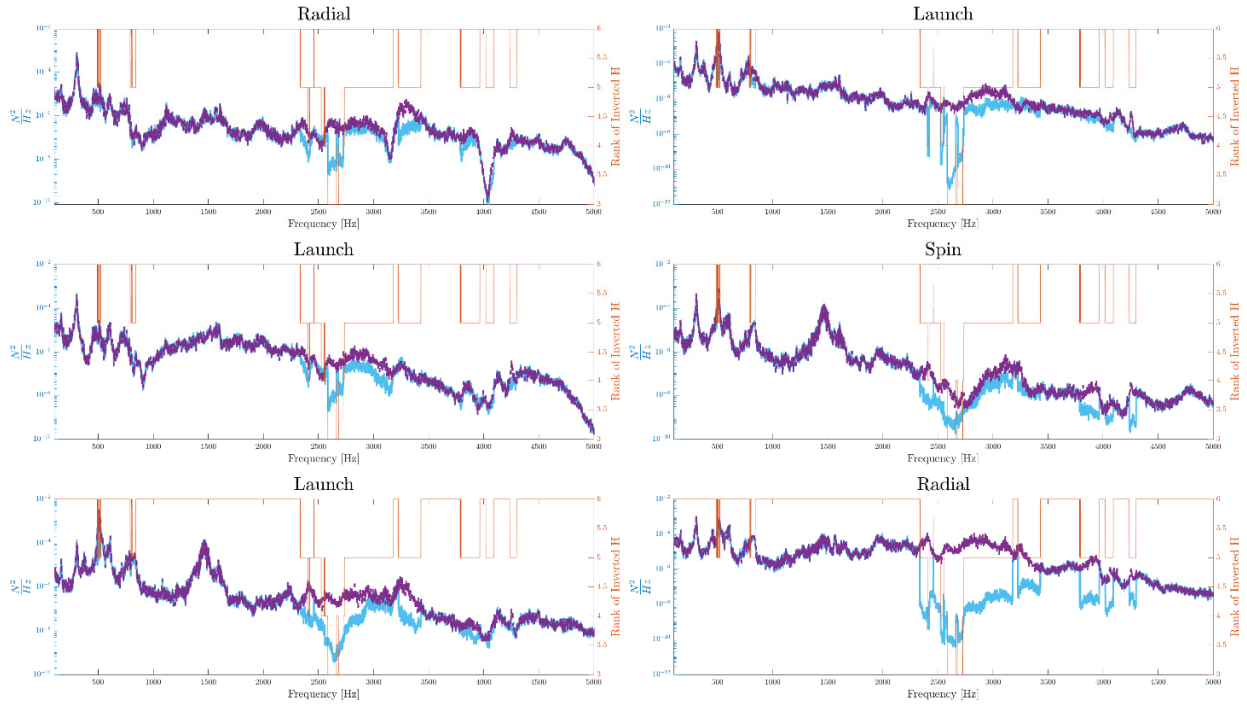
Figure 7*: Simulated forcing input ASD's for Configuration B with a threshold (blue) and without a threshold (purple)*

As predicted, the forcing input ASD's computed with the threshold are lower in magnitude when $H_{XF}^+(\omega)$ is truncated to be of rank less than full. Interestingly, the condition number threshold only affects the forces in a relatively small fraction of the frequency band. This effect is largest in the bandwidth from 2500 Hz to 3000 Hz. Looking at the modal data for Configuration B, its observed that there are axisymmetric (chip) plate modes at 2600 Hz and 2700 Hz along with a symmetric (bubble) plate mode at 3000 Hz. In fact, at the frequency lines where the rank of $H_{XF}^+(\omega)$ is less than full, there is always a mode of the assembly nearby. Therefore, the implementation of a condition number threshold in simulation effectively limits the forcing input magnitude near modes of the assembly under test. Similarly, because resonant frequencies of the assembly shift between operation and test, the physical closed loop control also drives down the input magnitude near the system's resonances. This case study shows that the use of condition number thresholds does have a relatively important effect on the MIMO test and should be used in any simulations.

7. Conclusions

This paper further investigated the influence of impedance on the ability to reconstruct a random vibration environment for a component by controlling to accelerometers only on a transmission simulator that the component is attached to. Prior work [11] suggested that a improved impedance match leads to a more accurate reconstruction response of the uncontrolled subcomponent. This research further examined the impact of impedance by analyzing a next-level assembly, Configuration C.

Configuration C included more of the operational structure than the previous two assemblies that had been studied. The results showed that the test was fairly accurate in reconstructing the environment on the TS in the launch direction, but there was significant deviation from the control in the off-launch directions. As a result, this translated to poor reconstruction accuracy on the uncontrolled stool. Comparing this configuration to the previous two assemblies, it was noted that although Configuration C included more of the operational structure and was presumed to have an improved impedance match, there was a degradation in accuracy on both the TS and the subcomponent of interest. This contradicted the assumptions from the previous work that suggested using more of the operational structure leads to a more successful response reconstruction test.

As a result of this finding, there are a few considerations to address moving forward. First, with increasingly complex assemblies under test, there is a need to explore metrics or concepts that can be used to quantify the difficulty of controlling a particular assembly. In this work we computed the number of flexible modes of the assembly and presented that as one possible metric. It appears that this consideration must be balanced with the impedance match when defining a TS for a particular application, as there are certainly cases where the TS can be too rigid to provide accurate results. The TS and fixture should be selected to capture only the modes that contribute most to the operational response, instead of simply choosing a fixture that contains the most operational modes.

Lastly, to improve upon the ability of MIMO simulations to predict physical MIMO tests, a condition number threshold was implemented. This approach decreased the magnitude of the inverted FRF thereby also limiting the amplitude of the forcing input, similar to what is done in real MIMO tests. Because the FRFs are ill-conditioned near the natural frequencies of the system under test, this approach drives down the input magnitudes at these frequencies. Comparing the error metrics between simulation and physical test, the simulations with the threshold implementation were consistently more predictive of the physical test.

Future work will investigate methods to quantify controllability and impedance while also exploring protocols for determining the dominant modes a TS and testing fixture should capture.

References

[1] Piersol, A., "The development of vibration test specifications for flight vehicle components," *J. Sound Vib.*, pp. 88–115, 1965.

[2] National Aeronautics and Space Administration, "Force Limited Vibration Testing," NASA-HDBK-7004B, 2003. [Online]. Available: http://standards.nasa.gov

[3] Paripovic, J and Mayes, Randall L., "Reproducing a component field environment on a six degree-of-freedom shaker," presented at the The 38th International Modal Analysis Conference (IMAC XXXVIII), Houston, TX, 2020.

[4] P. M. Daborn, C. Roberts, D. J. Ewins, and P. R. Ind, "Next-generation random vibration tests," 2014, vol. 8, pp. 397–410. doi: 10.1007/978-3-319-04774-4_37.

[5] R. L. Mayes and D. P. Rohe, "Physical Vibration Simulation of an Acoustic Environment with Six Shakers on an Industrial Structure," in *Shock & Vibration, Aircraft/Aerospace, Energy Harvesting, Acoustics & Optics, Volume 9*, 2016, pp. 29–41.

[6] C. Schumann, M. S. Allen, M. Tuman, W. DeLima, and E. Dodgen, "Transmission Simulator Based MIMO Response Reconstruction," *Exp. Tech.*, May 2021, doi: 10.1007/s40799-021-00454-4.

[7] Scharton, T.D., "Force Limited Vibration Testing Monograph," NASA, RP-1403, 1997.

[8] D. J. Segalman *et al.*, "Handbook on Dynamics of Jointed Structures," Sandia National Laboratories, Albuquerque, NM 87185, 2009.

[9] D. R. Roettgen and M. S. Allen, "Nonlinear characterization of a bolted, industrial structure using a modal framework," *Mech. Syst. Signal Process.*, vol. 84, pp. 152–170, 2017, doi: 10.1016/j.ymssp.2015.11.010.

[10] T. Van Fossen and K. Napolitano, "An Acceleration-Based Approach to Force Limiting a Random Vibration Test," in *Special Topics in Structural Dynamics & Experimental Techniques, Volume 5*, Cham, 2021, pp. 315–325.

[11] M. J. Tuman, C. A. Schumann, M. S. Allen, W. DeLima, and E. Dodgen, "Investigation of Transmission Simulator Based Response Reconstruction Accuracy," presented at the IMAC XXXIX, Virtual, 2021.

[12] C. A. Schumann, M. S. Allen, W. DeLima, and E. Dodgen, "Transmission Simulator Based MIMO Response Reconstruction for Vehicle Subcomponents," presented at the IMAC XXXVIII, Houston, TX, 2020.

[13] G. D. Nelson, D. P. Rohe, and R. A. Schultz, "Strategies for shaker placement for impedance-matched multi-axis testing," presented at the IMAC XXXVII, Orlando, FL, 2019.